Mammalian NADH diphosphatases of the Nudix family: cloning and characterization of the human peroxisomal NUDT12 protein

Salama R. ABDELRAHEIM*, David G. SPILLER† and Alexander G. McLENNAN*[1]

*Cell Regulation and Signalling Group, School of Biological Sciences, University of Liverpool, Liverpool L69 7ZB, U.K., and †Centre for Cell Imaging, School of Biological Sciences, University of Liverpool, Liverpool L69 7ZB, U.K.

The human NUDT12 Nudix hydrolase has been expressed in insect cells from a baculovirus vector as a His-tagged recombinant protein. *In vitro*, it efficiently hydrolyses NAD(P)H to NMNH and AMP (2′,5′-ADP), and diadenosine diphosphate to AMP. It also has activity towards $NAD(P)^+$, ADP-ribose and diadenosine triphosphate. K_m values for NADH, NADPH and NAD^+ are 11, 16 and 190 μM and k_{cat} values are 11, 16 and 10.5 s^{-1} respectively. Thus, like other NADH diphosphatases of the Nudix family, NUDT12 has a marked substrate preference for the reduced nicotinamide nucleotides. Optimal activity was supported by 50 μM Mn^{2+} ions *in vitro*, with 3-fold lower activity at 0.4 mM Mg^{2+}. Expression of NUDT12 as a C-terminal fusion to green fluorescent protein revealed that it was targeted to peroxisomes by the C-terminal tripeptide PNL acting as a novel type 1 peroxisomal targeting signal. Deletion of PNL resulted in diffuse cellular fluorescence. In addition, C-terminal, but not N-terminal, fusions with or without the PNL signal accumulated in large, unidentified cytoplasmic structures. NUDT12 may act to regulate the concentration of peroxisomal nicotinamide nucleotide cofactors required for oxidative metabolism in this organelle.

Key words: baculovirus, nucleotide metabolism, Nudix hydrolase, pyrophosphatase.

INTRODUCTION

Nucleotides are involved in numerous biochemical reactions and pathways within the cell as substrates, cofactors and effectors, a fact that reflects their ancient origin. Regulation of the concentrations of individual nucleotides and of nucleotide ratios in response to changing circumstances is clearly essential for cellular function. Prominent among the enzymes responsible for metabolizing nucleotides are the Nudix hydrolases. These enzymes are characterized by a distinctive catalytic motif, the Nudix or MutT motif, and act upon a wide range of substrates including (d)NTPs, nicotinamide nucleotides, CoA, dinucleoside polyphosphates and nucleotide sugars [1–3]. More recently, non-nucleotide compounds such as diphosphoinositol polyphosphates and phosphoribosyl pyrophosphate have been added to the repertoire of substrates [4–7]. Catalysis usually involves cleavage of a diphosphate (PP_i) bond, thus permitting nucleotide moieties to be recycled.

The Nudix hydrolases can be divided into subfamilies with particular sequence motifs that may contribute to substrate specificity [2]. Thus the sequence $LLTxR[SA]x_3Rx_3Gx_3FPGG$, designated UPF0035 in the PROSITE database and located immediately upstream of the Nudix motif, is found in hydrolases that prefer CoA and CoA esters as substrates [8–10]. Similarly, the sequence SQPWPFPxS is found a short distance downstream of the Nudix motif in hydrolases characterized as NADH diphosphatases from *Escherichia coli* [11], *Saccharomyces cerevisiae* [12,13] and *Caenorhabditis elegans* [13] and in many other sequences from other organisms that are therefore predicted to be NADH diphosphatases [2]. The human genome contains two Nudix genes, designated *NUDT12* and *NUDT13*, predicted to encode NADH diphosphatases according to the above criterion. The present study describes the cloning and characterization of NUDT12, a peroxisomal NADH diphosphatase.

MATERIALS AND METHODS

Materials

The DKFZp761l172Q3 human brain amygdala cDNA clone in the vector pSPORT1 was obtained from the RZPD Deutsches Resourcenzentrum für Genomforschung (Berlin-Charlottenburg, Germany; http://www.rzpd.de). The Bac-to-Bac HT baculovirus expression system (comprising the pFastBac HT vectors and competent *E. coli* DH10Bac containing the parent bacmid and helper plasmid), *E. coli* TOP10, Sf21 (*Spodoptera frugiperda*) and High Five™ (*Trichoplusia ni*) insect cells, Cellfectin, Sf-900 II serum-free medium (SFM) and TC-100 medium were obtained from Invitrogen (Paisley, U.K.). EX-CELL 405 medium was obtained from JRH Biosciences (St. Albans, Herts., U.K.) and pEGFP-N1 and pEGFP-C2 were from BD Biosciences Clontech (Oxford, U.K.). The anti-His-tag monoclonal antibody was obtained from Novagen (Nottingham, U.K.). LysoTracker Red DND-99 was from Molecular Probes Europe BV (Leiden, The Netherlands) and FuGENE™ was from Roche Diagnostics Ltd. (Lewes, Sussex, U.K.).

Construction of NUDT12 expression bacmid

NUDT12 was amplified from the clone DKFZp761l172Q3 by PCR using the forward and reverse primers 5′-CTTTGGGATCCAATGTCTTCTGTA-3′ and 5′-TCAGAGTCGACTGACCCAAAT-3′. These primers provided a *Bam*HI site at the start of

Abbreviations used: Ap_2A, diadenosine 5′,5‴-P^1,P^2-diphosphate; Ap_3A, diadenosine 5′,5‴-P^1,P^3-triphosphate; DTT, dithiothreitol; EGFP, enhanced green fluorescent protein; LB, Luria–Bertani; MEM, minimal essential medium; MOI, multiplicity of infection; $NAADP^+$, oxidized nicotinic acid–adenine dinucleotide phosphate; PTS1, peroxisomal targeting signal type 1; SFM, serum-free medium.

[1] To whom correspondence should be addressed (e-mail agmclen@liv.ac.uk).

the amplified gene and a *Sal*I site at the end. After amplification with *Pfu* DNA polymerase, the *NUDT12* PCR product was purified using a Qiagen PCR purification kit and digested with *Bam*HI and *Sal*I. The digest was gel-purified and the product ligated between the *Bam*HI and *Sal*I sites of the pFastBac HTa vector. The resulting pFast-NUDT12 construct (10 ng), encoding *NUDT12* with an N-terminal His-tag fusion under the control of the polyhedrin promoter, was electroporated into *E. coli* TOP10 cells for propagation and its structure confirmed by sequencing. A 0.1 ml aliquot of *E. coli* DH10Bac was mixed with 10 ng of pFast-NUDT12 and kept on ice for 45 min. The cells were then heat-shocked at 42 °C for 90 s and chilled for 5 min. The transformed cells were diluted into 0.9 ml of SOC medium. After 5 h incubation at 37 °C in SOC medium, the transformed DH10Bac cells were serially diluted with SOC medium and 100 μl of each serial dilution was plated on Miller Luria–Bertani (LB) agar plates containing 50 μg/ml kanamycin, 7 μg/ml gentamicin, 10 μg/ml tetracycline, 100 μg/ml Bluogal and 50 μg/ml isopropyl-1-thio-β-D-galactopyranoside. After 24 h incubation at 37 °C, a white colony containing the recombinant *NUDT12*-bacmid DNA was selected and re-streaked on a Miller LB agar plate containing the above components to confirm its white morphology [14]. This colony was used to inoculate 3 ml of LB containing 50 μg/ml kanamycin, 7 μg/ml gentamicin and 10 μg/ml tetracycline, which was then incubated for 16 h at 37 °C. Recombinant *NUDT12*-bacmid DNA was isolated using a CONCERT high-purity DNA purification kit (Life Technologies, Paisley, Renfrewshire, Scotland, U.K.) according to the manufacturer's instructions for the preparation of high-molecular-mass DNA and dissolved in TE buffer. Transposition of *NUDT12* into the bacmid DNA was confirmed by PCR.

Transfection of Sf21 cells with recombinant *NUDT12*-bacmid DNA

Sf21 cells (0.6×10^6) were seeded into a 35 mm dish at 27 °C. Recombinant *NUDT12*-bacmid DNA (6 μl) was diluted with 200 μl of Sf-900 II SFM containing 5 μl of Cellfectin and incubated at room temperature (22 °C) for 30–45 min. After dilution to 1 ml with Sf-900 II SFM, the transfection mixture was added in drops to washed Sf21 cells and the cells were incubated for 5 h at 27 °C. The cells were then incubated for 72 h at 27 °C in 2 ml of complete TC-100 medium [containing 10 % (v/v) foetal bovine serum], after which the supernatant containing recombinant *NUDT12* baculovirus was harvested, titrated and amplified [14].

Expression and purification of NUDT12

High Five™ cells were seeded as a monolayer in 20×75 mm^2 flasks at 10^7 cells/flask at 27 °C, then infected with recombinant *NUDT12* virus at a multiplicity of infection (MOI) of 10. After 72 h, the cells were dislodged, centrifuged at 1000 ***g*** for 10 min at 4 °C and then washed with PBS. The cells were lysed in 5 ml of a buffer containing 50 mM Tris/HCl (pH 8), 50 mM NaCl, 1 % (v/v) Nonidet P40, 1 mM dithiothreitol (DTT) and 1 mM PMSF, and the lysate was sonicated four times, for 30 s each time. The lysate was then clarified by centrifugation at 20 000 ***g*** for 20 min at 4 °C. The supernatant was mixed with 1 ml of NiCAM™-HC resin (Sigma) equilibrated in 50 mM Tris/HCl (pH 8.0)/500 mM NaCl and was gently shaken for 2 h at 4 °C. The mixture was then poured into a 15 mm × 50 mm column. The column was washed with 15 ml of wash buffer [50 mM Tris/HCl (pH 8.0)/500 mM NaCl/10 mM imidazole] and the protein was eluted with 3 ml of elution buffer [50 mM Tris/HCl (pH 8.0)/500 mM NaCl/0.25 M imidazole]. The purified protein was dialysed overnight against 2×1 litre of a buffer containing 50 mM Tris/HCl (pH 8.0), 50 mM NaCl and 1 mM DTT.

Enzyme assays

The standard colorimetric assay (200 μl) was incubated at 37 °C for 20 min and contained 50 mM Tris/HCl (pH 8.5), 0.4 mM $MgCl_2$, 1 mM DTT, 0.25 mM substrate, 0.1 μg of NUDT12 and 0.5 μg (1 unit) of alkaline phosphatase for phosphodiester substrates or 0.5 μg (100 m-units) of inorganic pyrophosphatase for phosphomonoesters. Phosphate released was determined colorimetrically [15]. Reaction products were identified by high-performance ion-exchange chromatography after incubation of 0.25 mM substrate with 0.15 μg of NUDT12 in 100 μl of 50 mM Tris/HCl (pH 8.5)/0.4 mM $MgCl_2$/1 mM DTT at 37 °C for 10 min [12]. Kinetic constants were determined from HPLC data obtained under these conditions using a range of substrate concentrations from 0.0025 to 3 mM and from 0.02 to 0.2 μg of enzyme.

NUDT12–enhanced green fluorescent protein (EGFP) fusion constructs and subcellular localization

NUDT12 was amplified from clone DKFZp761l172 by PCR using the same forward primer, 5′-TTGCTCGAGAATGTCTTCTGTAAAAAGAAGTCTG-3′, and any one of the reverse primers 5′-ACTCAAAGCTTAGTTCTTAG-3′, 5′-GATTTAAAGCTTTCAATTTATTCTAATCCAGTGTTT-3′ or 5′-GTTCTTAAAGCTTGAGATTAGGATTTATTCTAATCC-3′ to give PCR products 'C' (1421 bp), 'CΔPNL' (1402 bp) or 'N' (1409 bp) respectively. These primers provided an *Xho*I restriction site at the start of the amplified gene and a *Hin*dIII restriction site at the end. PCR products 'C' and 'CΔPNL' were cloned as C-terminal fusions to EGFP in the mammalian expression vector pEGFP-C2, whereas PCR product 'N', with the deletion of the *NUDT12* termination codon, was cloned as an N-terminal fusion to EGFP in pEGFP-N1. After amplification with *Pfu* DNA polymerase, the DNA products were recovered using a Qiagen PCR purification kit and digested with *Xho*I and *Hin*dIII. The digested PCR products 'C' and 'CΔPNL' were gel-purified and ligated between the *Xho*I and *Hin*dIII sites of pEGFP-C2 to give pEGFP-NUDT12 and pEGFP-NUDT12ΔPNL respectively. The digested PCR product 'N' was gel-purified and ligated into pEGFP-N1 to give pNUDT12-EGFP. The plasmids were propagated by transformation of *E. coli* TOP10 cells. HeLa cells (6×10^4 cells/dish) were seeded into 35 mm glass-bottomed dishes (MatTek, Ashland, MA, U.S.A.) in 2 ml of complete minimal essential medium (MEM; containing 10 % foetal bovine serum and non-essential amino acids) and transfected after 24 h when at 50 % confluence. FuGENE™ (2.5 μl/μg DNA) was diluted with 100 μl of serum-free MEM, incubated for 5 min at room temperature and added dropwise to 1–2 μg of each DNA construct, namely pNUDT12-EGFP, pEGFP-NUDT12, pEGFP-NUDT12ΔPNL or a 1:1 mixture of pEGFP-NUDT12 and pDsRed1-C1-mNudt7 DNA [8] in a volume of 10 μl. The mixture was incubated for 45 min at room temperature. The old medium was removed and replaced with 2 ml of fresh complete MEM and the transfection mixture was added dropwise to the cell monolayer. The cells were then incubated for up to 72 h at 37 °C in a humidified incubator containing 5 % CO_2. The subcellular localization of the expressed proteins was determined using a Zeiss LSM510 confocal microscope with a 100 × 1.4 NA

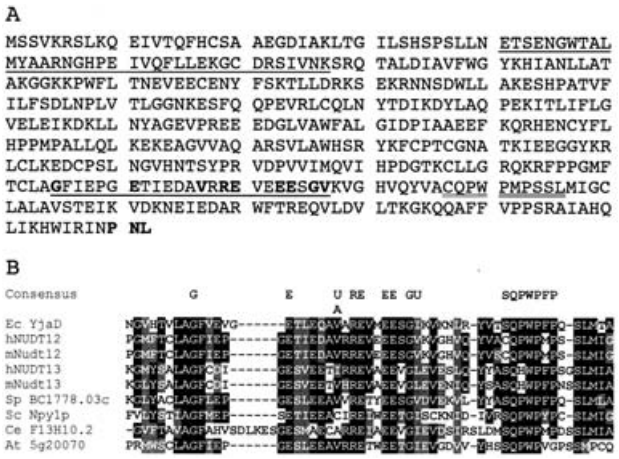

Figure 1 The NUDT12 protein sequence

(**A**) The consensus Nudix motif is underlined with the conserved residues in boldface; the downstream sequence indicative of NADH diphosphatases is double underlined; the ankyrin repeat near the N-terminus is underlined. (**B**) Partial sequence alignment of NUDT12 with related sequences (GenBank® accession numbers given in parentheses): *E. coli* YjaD (NP_756807); hNUDT12 (NP_113626); mNudt12 (BAB22253); hNUDT13 (XP_032512); mNudt13 (BAB29203); *Schiz. pombe* SPBC1778.03c (NP_596286); *S. cerevisiae* Npy1p (P53164); *C. elegans* F13H10.2 (NP_502051); *A. thaliana* At5g20070 (NP_197507).

objective. Lysosomes were visualized by incubating the HeLa cells 24–48 h after transfection with pEGFP-NUDT12 or pEGFP-NUDT12ΔPNL with MEM containing 100 nM LysoTracker Red DND-99 for 30–60 min at 37 °C in a humidified incubator in 5 % CO_2. After removal of the dye, cells were observed in the confocal microscope using appropriate laser excitation and filters. For green fluorescent protein, these were 488 nm excitation from an argon ion laser, with emission collected through a 505–530 nm band pass filter and, for DsRed and LysoTracker dye, these were 543 nm excitation with an He–Ne laser and collection from a 545 nm dichroic mirror through a 585 nm long pass filter.

RESULTS

The NUDT12 sequence

The *NUDT12* gene on chromosome 5q21 encodes the open reading frame of the putative 462-amino-acid, 52 kDa NUDT12 protein (GenBank® Nucleotide Sequence Database accession no. NP_113626; Figure 1A). This open reading frame has a perfect consensus Nudix motif and the downstream sequence CQPWPMPSS, which suggests that NUDT12 is probably an NADH diphosphatase [2,13]. In addition, a single ankyrin repeat sequence in the N-terminal region is annotated as such in GenBank®. Figure 1(B) shows a partial sequence alignment of the region of Nudix and SQPWPFPxS motifs of human NUDT12 (hNUDT12) and the mouse orthologue (88 % identity, 94 % similarity), mouse Nudt12 (mNudt12) with *E. coli* YjaD, hNUDT13 and mNudt13, *S. cerevisiae* Npy1p and *C. elegans* F13H10.2 (both of which are known NADH diphosphatases) and the related *Schizosaccharomyces pombe* BC1778.03c and *Arabidopsis thaliana* At5g20070 proteins. The *NUDT13* gene on chromosome 10q22.3 encodes a second, distinct mitochondrial NADH diphosphatase, which has 45 % identity and 60 % similarity to NUDT12 in the C-terminal half (S. R. AbdelRaheim and A. G. McLennan, unpublished work).

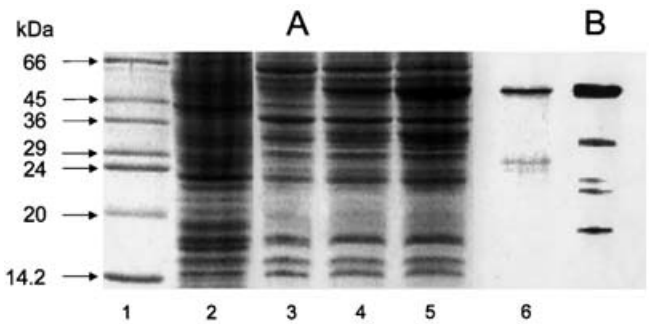

Figure 2 Expression of NUDT12 in High Five™ cells and purification

High Five™ cells were infected with recombinant NUDT12 virus at an MOI of 10. Samples were taken at 24, 48 and 72 h after infection, boiled in SDS sample buffer and then analysed by SDS/PAGE (15 % gel, w/v) followed by staining with Coomassie Blue. (**A**) Lane 1, protein standards: BSA (66 kDa), ovalbumin (45 kDa), glyceraldehyde-3-phosphate dehydrogenase (36 kDa), carbonic anhydrase (29 kDa), trypsinogen (24 kDa), soya-bean trypsin inhibitor (20 kDa) and α-lactalbumin (14.2 kDa). Lane 2, total cell extract of control uninfected High Five™ cells. Lanes 3–5, total cell extracts of High Five™ cells infected with recombinant NUDT12 virus at 24, 48 and 72 h respectively. Lane 6, purified NUDT12. (**B**) Immunoblot analysis of the expressed NUDT12 (the same cells as in **A**, lane 5) using an anti-His-tag monoclonal antibody.

Cloning of *NUDT12* in baculovirus, and expression and purification of NUDT12

Initial attempts to produce soluble, active recombinant NUDT12 from pET15b, pET17b and pET32b vectors in *E. coli* BL21(DE3) were unsuccessful. However, high yields were obtained using a Bac-to-Bac baculovirus expression system. The *NUDT12* sequence was PCR-amplified from a full-length human brain amygdala cDNA clone and inserted between the *Bam*HI and *Sal*I sites of the pFastBac HTa expression vector so that the protein would be expressed with the His tag at its N-terminus, giving a protein of expected molecular mass 55.5 kDa. The pFast-NUDT12 DNA construct was transformed into DH10Bac *E. coli* containing parent bacmid DNA and the pFast-NUDT12 DNA was allowed to transpose into the bacmid DNA. Recombinant NUDT12-bacmid DNA was then prepared and amplified to a titre of 1×10^8 pfu (plaque-forming units)/ml in Sf21 insect cells. High Five™ insect cells were then infected with the NUDT12 viral supernatant at an MOI of 10 and samples were taken 24, 48 and 72 h after infection. Uninfected cells were also processed 72 h after plating. Analysis by SDS/PAGE showed an increase in the synthesis of a 55 kDa protein, reaching a maximum 48–72 h after infection with the NUDT12 virus. This was assumed to be the desired product (Figure 2A). The identity of the protein was confirmed by Western blotting using an anti-His-tag monoclonal antibody, which detected the N-terminal His tag of the recombinant NUDT12 as the major protein on the blot (Figure 2B). The minor bands may be proteolytic products of NUDT12 or endogenous *E. coli* proteins containing clusters of His residues. Interestingly, a significant amount (approx. 1 %) of the NUDT12 was secreted into the growth medium, where it could be readily assayed. NUDT12 protein was purified from a large-scale infection of High Five™ cells using NiCAM™-HC resin as described in the Materials and methods section (Figure 2A, lane 6).

Substrate specificity of NUDT12

NUDT12 was found to be active towards nicotinamide nucleotides, diadenosine polyphosphates and ADP-ribose when a wide range of substrates was assayed at a fixed concentration of

Table 1 Substrate specificity of NUDT12

Substrate specificity of NUDT12 was determined colorimetrically at a fixed substrate concentration of 0.25 mM. The activity was expressed relative to NADH hydrolysis under the same conditions, where 100 % was 11.5 μmol NADH hydrolysed · min^{-1} · (mg protein)$^{-1}$. Values are the averages of duplicate determinations.

Substrate	Relative activity (%)	Substrate	Relative activity (%)
NADH	100	Ap_3A	44
NADPH	136	Ap_4A	22
NAD^+	59	Ap_5A	13
$NADP^+$	63	Ap_6A	9
Desamido NAD^+	35	dGTP	3.8
$NAADP^+$	17	dATP	4.9
FAD	63	ADP	2
ADP-ribose	57	AMP	0.2
Ap_2A	75		

Table 2 Kinetic parameters for NUDT12-catalysed nucleotide hydrolysis

The enzyme obeyed Michaelis–Menten kinetics with all substrates. Kinetic constants were determined by non-linear regression analysis.

Substrate	K_m (μM)	V_{max} (μmol · min^{-1} · mg^{-1})	k_{cat} (s^{-1})	k_{cat}/K_m (10^6 M^{-1} · s^{-1})
NADH	11	12	11	1.0
NADPH	16	17	16	1.0
NAD^+	190	11.5	10.5	0.055

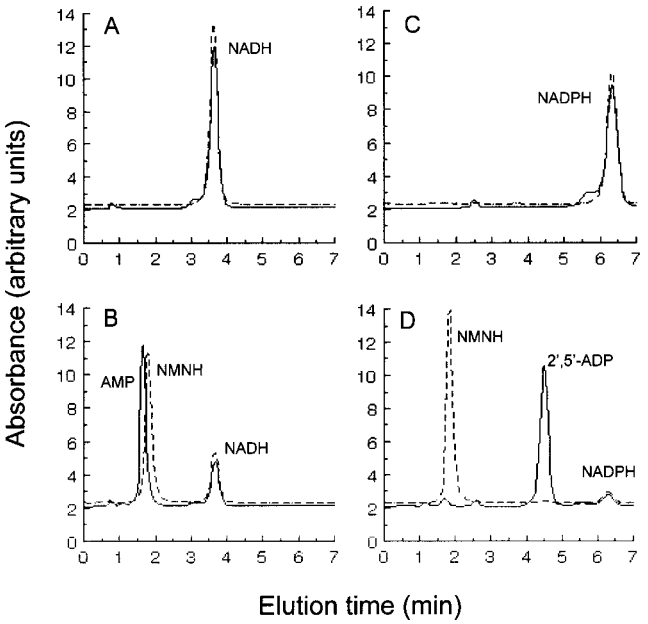

Figure 3 Determination of reaction products of NADH and NADPH hydrolysis by NUDT12

The reaction mixtures, containing 0.25 mM NADH (**A**, **B**) or NADPH (**C**, **D**), were incubated at 37 °C for 10 min without (**A**, **C**) or with (**B**, **D**) NUDT12 (0.15 μg) and the reaction products were separated by HPLC. ——, Absorbance at 259 nm; – – –, absorbance at 340 nm.

0.25 mM. High activity was observed with NADPH, NADH and diadenosine 5′,5‴-P^1,P^2-diphosphate (Ap_2A). Moderate activity was observed with FAD, $NADP^+$, NAD^+, ADP-ribose and diadenosine 5′,5‴-P^1,P^3-triphosphate (Ap_3A). Low activity was observed with deamido NAD^+, oxidized nicotinic acid–adenine dinucleotide phosphate ($NAADP^+$) and other diadenosine polyphosphates. Minimal activity was observed with deoxynucleoside 5′-triphosphates, nucleoside 5′-diphosphates and nucleoside 5′-monophosphates (Table 1). These results suggested that NADH and NADPH are the best substrates of NUDT12. This was confirmed by determination of K_m and k_{cat} values (Table 2). From the specificity constant k_{cat}/K_m, it is evident that NADH is preferred to NAD^+ by a factor of 20, due mainly to the 20-fold lower K_m value for NADH, whereas the enzyme shows little discrimination between NADH and NADPH. The strong preference for reduced nicotinamide nucleotides seems to be a common feature of this class of enzymes [11,13].

Reaction requirements of NUDT12

With NADH as substrate, NUDT12 displayed optimal activity at alkaline pH, between pH 8 and 9, with approx. 50 % activity remaining at pH 6.5 and 11.0. The enzyme was absolutely dependent on a bivalent metal cation for its activity. Maximum activity was achieved with 50 μM $MnCl_2$, with 3-fold lower activity obtained between 0.4 and 2 mM $MgCl_2$. Kinetic parameters were obtained in 0.4 mM $MgCl_2$ as this may be more physiologically relevant.

Product analysis

To determine the products of NADH, NADPH, NAD^+, $NADP^+$, Ap_2A, Ap_3A and ADP-ribose hydrolysis, aliquots of reaction mixtures containing each substrate were analysed by ion-exchange HPLC. Disappearance of substrate was accompanied by the appearance of AMP and NMNH for NADH (Figure 3B) and by 2′,5′-ADP and NMNH for NADPH (Figure 3D). Similar analyses of other nucleotides showed the products to be: NAD^+, AMP and NMN^+ (presumed); ADP-ribose, AMP and ribose-5-phosphate (presumed); $NADP^+$, 2′,5′-ADP and NMN (presumed); Ap_2A, AMP (2 mol); and Ap_3A, AMP and ADP. Presumed products could not be detected by UV absorption.

Subcellular localization of NUDT12

S. cerevisiae Npy1p is localized to peroxisomes by virtue of the C-terminal tripepetide SHL, a peroxisomal targeting signal type 1 (PTS1) [12]. The PTS1 consensus sequence is (S/A/C)-(K/R/H)(L/M) [16]. The C-terminal tripeptide of NUDT12 (and the mouse orthologue mNudt12) is PNL, which does not conform precisely to the PTS1 consensus. However, a hexadecapeptide terminating in PNL has been shown to interact with the human Pex5p PTS1 receptor, suggesting that it is a potential PTS1 [16]. Therefore expression plasmids encoding N-, C- or C-terminal with deleted PNL fusions of NUDT12 to EGFP were constructed by cloning *NUDT12* from a cDNA by PCR using the same forward primer and three different reverse primers to give PCR products ‘N’, ‘C’ and ‘CΔPNL’. The PCR product ‘N’ was ligated into pEGFP-N1, whereas the PCR products ‘C’ and ‘CΔPNL’ were ligated into pEGFP-C2 to give pNUDT12-EGFP, pEGFP-NUDT12 and pEGFP-NUDT12ΔPNL respectively. HeLa cells were transfected with these constructs and then examined by confocal microscopy. Cells transfected with pNUDT12-EGFP showed a diffuse, cytoplasmic fluorescence (Figure 4A), whereas cells transfected with pEGFP-NUDT12 showed a granular cytoplasmic fluorescence composed of intensely fluorescent small and large, rounded to oval spots (Figure 4B). Fluorescence was lost specifically from the small spots in cells transfected with pEGFP-NUDT12ΔPNL (Figure 4C). When the cells were co-transfected with pEGFP-NUDT12 and pDsRed1-C1-mNudt7, a

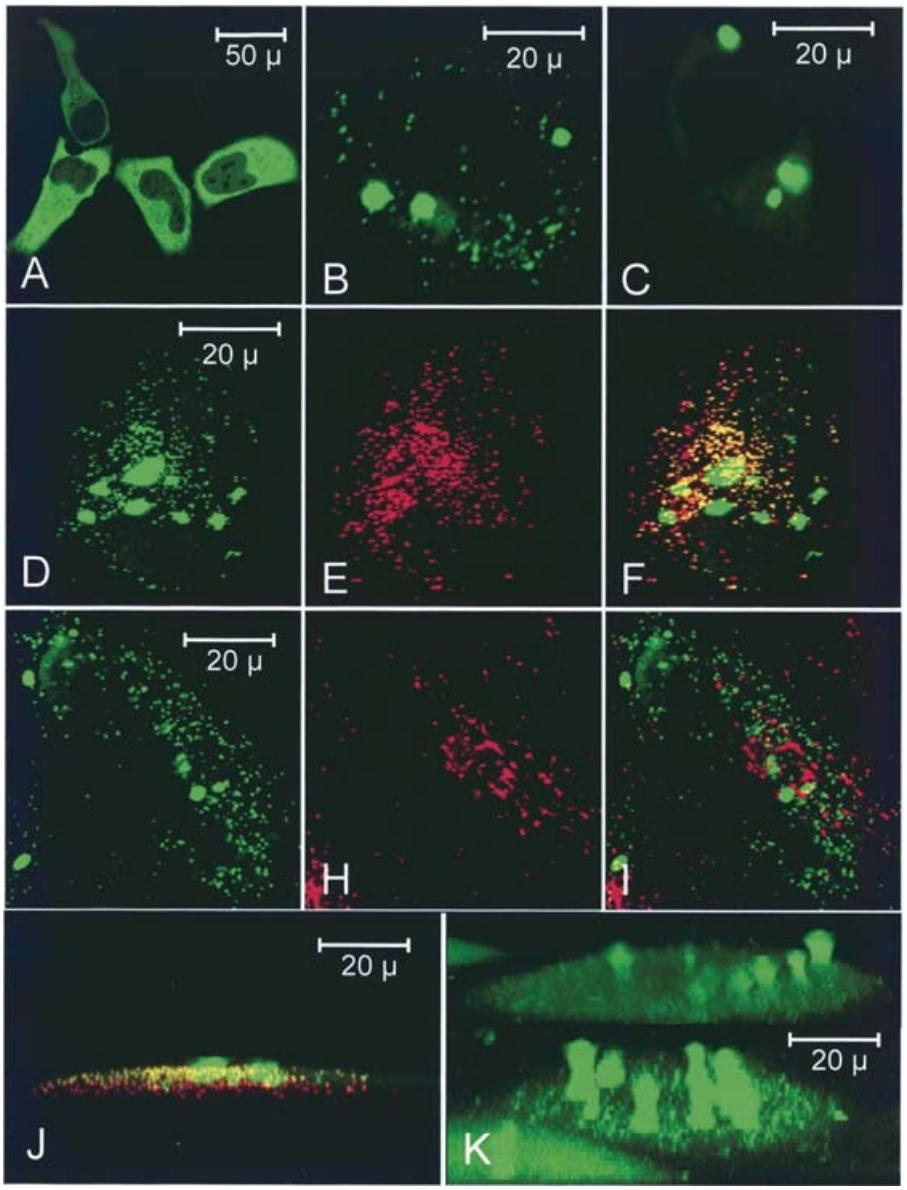

Figure 4 Subcellular localization of NUDT12 by fluorescence confocal microscopy

EGFP fluorescence of HeLa cells transfected with (**A**) pNUDT12-EGFP, (**B**) pEGFP-NUDT12 and (**C**) pEGFP-NUDT12ΔPNL. (**D**) EGFP fluorescence of a sample cell transfected with pEGFP-NUDT12. (**E**) Red fluorescence of the same cell in (**D**) co-transfected with pDsRed1-C1-mNudt7. (**F**) Superimposition of (**D**, **E**). (**G**) EGFP fluorescence of a sample cell transfected with pEGFP-NUDT12. (**H**) Red fluorescence of the cell in (**G**) stained with LysoTracker Red DND-99. (**I**) Superimposition of (**G**, **H**). (**J**) Lateral view of the cell in (**F**). (**K**) Lateral view of cells transfected with pEGFP-NUDT12 as in (**B**).

vector encoding the mNudt7 peroxisomal CoA diphosphatase fused to red fluorescent protein [8], the small green fluorescent spots (Figure 4D) co-localized with red fluorescent spots of the known peroxisomal protein (Figure 4E). Both signals from the small spots appeared coincident, as shown by the yellow fluorescence, but the large spots were clearly distinct from the peroxisomes (Figure 4F). Thus NUDT12 appears to be targeted to peroxisomes by the C-terminal tripeptide PNL acting as a novel PTS1. Interestingly, a lateral view of cells co-expressing both EGFP-NUDT12 and DsRed1-mNudt7 appeared to show an asymmetric distribution of two distinct populations of peroxisomes, with a subset expressing both fusion constructs forming a physically distinct layer above a subset expressing only DsRed1-mNudt7 (Figure 4J).

Specific staining of lysosomes with LysoTracker Red dye showed that the large structures containing EGFP–NUDT12 were not lysosomes. The red-staining lysosomes were quite distinct from both the peroxisomes and the large structures (Figures 4G–4I). Lateral views revealed these structures to be columnar, traversing a considerable part of the width of the cell. In some cases, due to the intensity of fluorescence, they seemed to project through the cell membrane (Figures 4J and 4K).

DISCUSSION

hNUDT12 is the first mammalian Nudix NADH diphosphatase to be cloned and characterized and it is one of two such enzymes with different subcellular locations found in mammalian cells. The

catalytic properties of NUDT12 are similar to those described previously for the Nudix NADH diphosphatases from *E. coli*, *S. cerevisiae* and *C. elegans*. NUDT12 preferentially hydrolyses a variety of 5′,5′-dinucleotide substrates containing two or three phosphate groups. It is most active with reduced nicotinamide nucleotides, preferring NADH to NAD^+ by a factor of 20. This ratio is 120, 60 and 30 for the enzymes from *E. coli*, *S. cerevisiae* and *C. elegans* respectively [11,13]. However, the K_m value for NADH of 11 μM is much lower than the K_m values reported for the other enzymes: 0.11 mM (*E. coli*), 1.6 mM (*S. cerevisiae*) and 1.4 mM (*C. elegans*), whereas the k_{cat} value of 11 s^{-1} in the presence of Mg^{2+} is similar to that for the other enzymes [11,13]. The optimal Mg^{2+} concentration under standard assay conditions of 0.4–2 mM is lower than the 5–10 mM optimum reported for *E. coli*, *S. cerevisiae* and *C. elegans* enzymes [11–13], which may be related to the higher nucleotide substrate affinity. Higher activity (3-fold) was obtained in the presence of 50 μM Mn^{2+} ions compared with 0.4 mM Mg^{2+}. Higher activity with Mn^{2+} has been noted for the *E. coli* [11] and *S. cerevisiae* [12] enzymes. In eukaryotes, cytosolic Mn^{2+} concentration is estimated to be as low as 10^{-8} M, although it can be 10–100-fold higher in vesicles and organelles into which it is actively transported [17]. Since Mn-dependent superoxide dismutase is present in peroxisomes [18], this organelle may contain a significant level of Mn^{2+} to maintain an enzyme-bound metal ion. However, it is doubtful whether free Mn^{2+} would be at a level sufficient to activate nucleotide hydrolysis by NUDT12 in the presence of competing Mg^{2+}. Hence, the preference for Mn^{2+} may simply be an *in vitro* property.

Recently, a Nudix NADH diphosphatase from *A. thaliana* was described in [19]. This is not the At5g20070 protein (Figure 1B) but the At1g68760 protein, which does not possess the characteristic SQPWPFPxS motif and which is the probable orthologue of the uncharacterized human Nudix hydrolase FLJ10956 (GenBank® accession no. NP_060753) on chromosome 13q14.11 with which it shares 43 % identity. Similar to NUDT12, At1g68760 has a 20-fold preference for NADH over NAD^+ in the presence of Mn^{2+}, although this is due to a 20-fold higher k_{cat} value for NADH rather than a 20-fold lower K_m value as is the case for NUDT12. The activity towards NADH was measured in the presence of 5 mM Mn^{2+}, which is unphysiological, so it is possible that it has a different substrate preference under more physiological conditions.

NUDT12 is localized to peroxisomes by the C-terminal tripeptide PNL, thus establishing PNL as a new *bona fide* PTS1 in human cells, a possibility suggested previously by the interaction of this tripeptide sequence with human Pex5p [16]. Peptides with potentially novel Pex5p-binding PTS1 sequences were found to possess predominantly hydrophobic residues 2 and 5 amino acids upstream of PTS1. Consistent with this, hNUDT12 has isoleucine and tryptophan residues and mNudt12 has methionine and tryptophan residues at these positions. The peroxisomal location of *S. cerevisiae* Npy1p has also been established experimentally, whereas *C. elegans* F13H10.2 has the C-terminal peptide SRI, very close to the SKI of the known *C. elegans* Y87G2A.14 peroxisomal CoA diphosphatase [9]. Thus it is quite probable that F13H10.2 is also peroxisomal. The C-terminal VKM of the *Schiz. pombe* SPBC1778.03c protein may also act as a PTS1 since both AKM and VKL bind to *S. cerevisiae* Pex5p [16], whereas the SSL found in the *A. thaliana* 5g20070 protein is known to act as a targeting signal for trypanosome glycosomes [20]. The occurrence of peroxisomal NADH diphosphatases appears, therefore, to be widespread. Regarding a possible function for this enzyme, deletion of the *S. cerevisiae NPY1* gene has yielded no obvious phenotype [12,13]. In a previous study [12], we suggested roles of this enzyme in the specific regulation of peroxisomal nucleotide cofactor coenzyme concentrations independent of those in other subcellular compartments or in the elimination of as yet unidentified and potentially toxic oxidized nucleotide metabolites generated within the peroxisomal environment. However, the true function is yet to be established.

The asymmetric distribution of peroxisomes seen in the lateral views of cells transfected with pEGFP-NUDT12 and pDsRed1-C1-mNudt7 also requires explanation. Peroxisomal heterogeneity is well established, with subsets differing in size, shape and protein composition [21,22]. This heterogeneity may extend to the location of different subsets, e.g. mature and immature, within the cell. One possibility is that peroxisomal subsets differ in their ability to recognize PNL as a PTS1: all recognize the prototypical SKL at the C-terminus of the mNudt7 CoA diphosphatase, but only a subset (immature?) recognizes the unusual PNL of NUDT12. Alternatively, it may be an experimental artifact. Again, this finding requires further investigation.

The nature of the large, columnar fluorescent structures seen in HeLa cells transfected with the pEGFP-NUDT12 construct is unknown. One possibility is that they represent aggregates of misfolded protein due to overexpression. However, large quantities of misfolded protein tend to be sequestered in a single, large pericentriolar cytoplasmic structure, termed as an aggresome, which looks quite different from the structures observed here [23,24]. Multiple cytoplasmic structures comprising protein aggregates, such as the interferon-induced protein called IFP35, have also been observed, but they tend to be much smaller then those observed in the present study and do not have the unusual columnar structure [25]. If these structures are aggregates, then aggregation may somehow involve the putative ankyrin repeat sequence near the N-terminus. Ankyrin repeats participate in both inter- and intramolecular protein interactions, although multiple repeats are usually present [26]. Alternatively, they may be the aborted products of an overloaded secretory pathway. A significant amount of the NUDT12 protein expressed from the baculovirus was found in the growth medium, although there were no obvious signs of cell disruption in the insect cells. Their shape does suggest something more than random protein aggregation and further work is required to establish their true nature and significance.

S. R. A. is the recipient of a scholarship from the Egyptian government. A. G. M. is supported by the Wellcome Trust. We are grateful to Carl Zeiss Ltd. (Welwyn Garden City, Herts., U.K.) and the Higher Education Funding Council for grants to the Centre for Cell Imaging (School of Biological Sciences, University of Liverpool).

REFERENCES

1 Bessman, M. J., Frick, D. N. and O'Handley, S. F. (1996) The MutT proteins or 'nudix' hydrolases, a family of versatile, widely distributed, 'housecleaning' enzymes. J. Biol. Chem. **271**, 25059–25062

2 Dunn, C. A., O'Handley, S. F., Frick, D. N. and Bessman, M. J. (1999) Studies on the ADP-ribose pyrophosphatase subfamily of the Nudix hydrolases and tentative identification of *trgB*, a gene associated with tellurite resistance. J. Biol. Chem. **274**, 32318–32324

3 McLennan, A. G. (1999) The MutT motif family of nucleotide phosphohydrolases in man and human pathogens. Int. J. Mol. Med. **4**, 79–89

4 Caffrey, J. J., Safrany, S. T., Yang, X. N. and Shears, S. B. (2000) Discovery of molecular and catalytic diversity among human diphosphoinositol-polyphosphate phosphohydrolases – an expanding Nudt family. J. Biol. Chem. **275**, 12730–12736

5 Leslie, N. R., McLennan, A. G. and Safrany, S. T. (2002) Cloning and characterisation of hAps1 and hAps2, human diadenosine polyphosphate-metabolising Nudix hydrolases. BMC Biochem. **3**, 20

6 Fisher, D. I., Safrany, S. T., Strike, P., McLennan, A. G. and Cartwright, J. L. (2002) Nudix hydrolases that degrade dinucleoside and diphosphoinositol polyphosphates also have 5-phosphoribosyl 1-pyrophosphate (PRPP) pyrophosphatase activity that generates the glycolytic activator ribose 1,5-bisphosphate. J. Biol. Chem. **277**, 47313–47317

7 Safrany, S. T., Ingram, S. W., Cartwright, J. L., Falck, J. R., McLennan, A. G., Barnes, L. D. and Shears, S. B. (1999) The diadenosine hexaphosphate hydrolases from *Schizosaccharomyces pombe* and *Saccharomyces cerevisiae* are homologues of the human diphosphoinositol polyphosphate phosphohydrolase – overlapping substrate specificities in a MutT-type protein. J. Biol. Chem. **274**, 21735–21740

8 Gasmi, L. and McLennan, A. G. (2001) The mouse *Nudt7* gene encodes a peroxisomal nudix hydrolase specific for coenzyme A and its derivatives. Biochem. J. **357**, 33–38

9 AbdelRaheim, S. and McLennan, A. G. (2002) The *Caenorhabditis elegans* Y87G2A.14 Nudix hydrolase is a peroxisomal coenzyme A diphosphatase. BMC Biochem. **3**, 5

10 Cartwright, J. L., Gasmi, L., Spiller, D. G. and McLennan, A. G. (2000) The *Saccharomyces cerevisiae PCD1* gene encodes a peroxisomal nudix hydrolase active towards coenzyme A and its derivatives. J. Biol. Chem. **275**, 32925–32930

11 Frick, D. N. and Bessman, M. J. (1995) Cloning, purification, and properties of a novel NADH pyrophosphatase – evidence for a nucleotide pyrophosphatase catalytic domain in MutT-like enzymes. J. Biol. Chem. **270**, 1529–1534

12 AbdelRaheim, S. R., Cartwright, J. L., Gasmi, L. and McLennan, A. G. (2001) The NADH diphosphatase encoded by the *Saccharomyces cerevisiae NPY1* nudix hydrolase gene is located in peroxisomes. Arch. Biochem. Biophys. **388**, 18–24

13 Xu, W. L., Dunn, C. A. and Bessman, M. J. (2000) Cloning and characterization of the NADH pyrophosphatases from *Caenorhabditis elegans* and *Saccharomyces cerevisae*, members of a Nudix hydrolase subfamily. Biochem. Biophys. Res. Commun. **273**, 753–758

14 O'Reilly, D. R., Miller, L. K. and Luckow, V. A. (1992) Baculovirus Expression Vectors: A Laboratory Manual, W. H. Freeman, New York

15 Canales, J., Pinto, R. M., Costas, M. J., Hernández, M. T., Miró, A., Bernet, D., Fernández, A. and Cameselle, J. C. (1995) Rat liver nucleoside diphosphosugar or diphosphoalcohol pyrophosphatases different from nucleotide pyrophosphatase or phosphodiesterase I: specificities of Mg^{2+}- and/or Mn^{2+}-dependent hydrolases acting on ADP-ribose. Biochim. Biophys. Acta **1246**, 167–177

16 Lametschwandtner, G., Brocard, C., Fransen, M., van Veldhoven, P., Berger, J. and Hartig, A. (1998) The difference in recognition of terminal tripeptides as peroxisomal targeting signal 1 between yeast and human is due to different affinities of their receptor Pex5p to the cognate signal and to residues adjacent to it. J. Biol. Chem. **273**, 33635–33643

17 Fraústo da Silva, J. J. R. and Williams, R. J. P. (2001) The Biological Chemistry of the Elements, 2nd edn, Oxford University Press, Oxford

18 Singh, A. K., Dobashi, K., Gupta, M. P., Asayama, K., Singh, I. and Orak, J. K. (1999) Manganese superoxide dismutase in rat liver peroxisomes: biochemical and immunochemical evidence. Mol. Cell. Biochem. **197**, 7–12

19 Dobrzanska, M., Szurmak, B., Wyslouch-Cieszynska, A. and Kraszewska, E. (2002) Cloning and characterization of the first member of the Nudix family from *Arabidopsis thaliana*. J. Biol. Chem. **277**, 50482–50486

20 de Hoop, M. J. and Ab, G. (1992) Import of proteins into peroxisomes and other microbodies. Biochem. J. **286**, 657–669

21 Schrader, M., Baumgart, E., Volkl, A. and Fahimi, H. D. (1994) Heterogeneity of peroxisomes in human hepatoblastoma cell line HepG2. Evidence of distinct subpopulations. Eur. J. Cell Biol. **64**, 281–294

22 Erdmann, R., Veenhuis, M. and Kunau, W. H. (1997) Peroxisomes: organelles at the crossroads. Trends Cell Biol. **7**, 400–407

23 Johnston, J. A., Ward, C. L. and Kopito, R. R. (1998) Aggresomes: a cellular response to misfolded proteins. J. Cell Biol. **143**, 1883–1898

24 Kopito, R. R. (2000) Aggresomes, inclusion bodies and protein aggregation. Trends Cell Biol. **10**, 524–530

25 Meyerdierks, A., Denecke, B., Rohde, M., Taparowsky, E. J. and Böttger, E. C. (1999) A cytoplasmic structure resembling large protein aggregates induced by interferons. J. Histochem. Cytochem. **47**, 169–182

26 Sedgwick, S. G. and Smerdon, S. J. (1999) The ankyrin repeat: a diversity of interactions on a common structural framework. Trends Biochem. Sci. **24**, 311–316

Received 20 March 2003/8 May 2003; accepted 5 June 2003
Published as BJ Immediate Publication 5 June 2003, DOI 10.1042/BJ20030441